Influence of different wind directions in relation to topography on the outbreak of convection in Northern England

J. Thielen, A. Gadian

Ann. Geophysicae 14, 1078–1087 (1996)

Annales Geophysicae

Influence of different wind directions in relation to topography on the outbreak of convection in Northern England

J. Thielen[1], A. Gadian[2]

[1] L.T.H.E., F-38041 Grenoble Cedex 09, France
[2] Department of Physics, UMIST, Manchester M60 1QD, UK

Received: 24 April 1995/Revised: 9 February 1996/Accepted: 21 February 1996

Abstract. The influence of different wind directions on the outbreak of convection in Northern England, was investigated with a high-resolution numerical model. The Clark model, a 3D finite-difference, non-hydrostatic model was used in this study. It was initialised with the topography of Northern England, a representation of surface characteristics, and used a routinely available meteorological sounding, typical of the unstable conditions. Results showed that convective cells were initially triggered in the lee of the elevated terrain, and that only after the convection had developed, were cells upwind of the elevated terrain produced. The windward slopes themselves seemed sheltered from convection. Under most wind directions, the central Pennines (the Forest of Trawden and the Forest of Rossendale) seemed particularly affected by convective rainfall.

1 Introduction

In Northern England the land has a width of approximately 200 km between the Irish Sea and North Sea. Centred between these coasts, the Pennines, a north-south-oriented ridge, have maximum elevations of up to 800 m, are on average 50 km wide, and represent a very structured terrain with deep and narrow valleys, mainly in east-west directions. The area, particularly around the central Pennines, i.e. the Forest of Rossendale to the Forest of Trawden, is affected by the combination of influences of land-sea contrasts, elevated terrain, and the presence of urban areas. All of these influences might potentially be important for the initiation and development of convection.

Numerous descriptions of convective storms in Northern England have seemed to indicate that the Pennines have influence on the development of convective rainfall (e.g. Acreman, 1989; Bader *et al*., 1983; Dent and Monk, 1983; Chaplain, 1983). For example, three storms, which rank amongst the 10 highest short-period rainfalls in Britain (Reynolds, 1978; Thielen, 1994), occurred within a radius of 30 km in the central Pennines. The location of the storm centres, Hewenden Reservoir, Walshaw Dean Lodge, and Ilkley, are marked in Fig. 1.

The concentration of particularly severe storms in the area of the central Pennines, has provoked research on the outbreak of convection in the north of England (Collinge and Acreman, 1991). Observational data from an extended gauge network, the Hameldon Hill C-band weather radar, meteorological routine soundings and weather maps were used to investigate several case studies of storms which caused much flood damage, such as the Hewenden reservoir storm (Collinge *et al*., 1992), and the Halifax storm (Collinge *et al*., 1990). Analyses of the data seemed to suggest that particularly the lower level winds around the Pennines were important for the outbreak and development of the storms. However, due to the lack of a large number of case studies and detailed meteorological data, no definite conclusions could be drawn. Thus, for this study, a numerical model was initialised with topography and surface characteristics of Northern England. It allowed the possible effects of orography, urban heat islands, sea breezes, and different wind directions on the initiation and development of convection in the vicinity of the Pennines to be studied. In Thielen (1994), for a southerly air flow regime only, the urban heat island forcing and the effects of surface topography were examined. The presence of large urban areas promoted enhancement of convection downstream, and there was evidence that topography tended to focus the tracks of convective cells. In this study, the development of convection under influence of different wind directions and uni-directional windshear is presented.

Convective storms have been a centre of interest of meteorological studies because of their vigorous nature and the often damaging effects for the environment (Ludlam, 1980). With increasing computing power, numerical simulations of severe convective storms have helped the

Correspondence to: A. Gadian

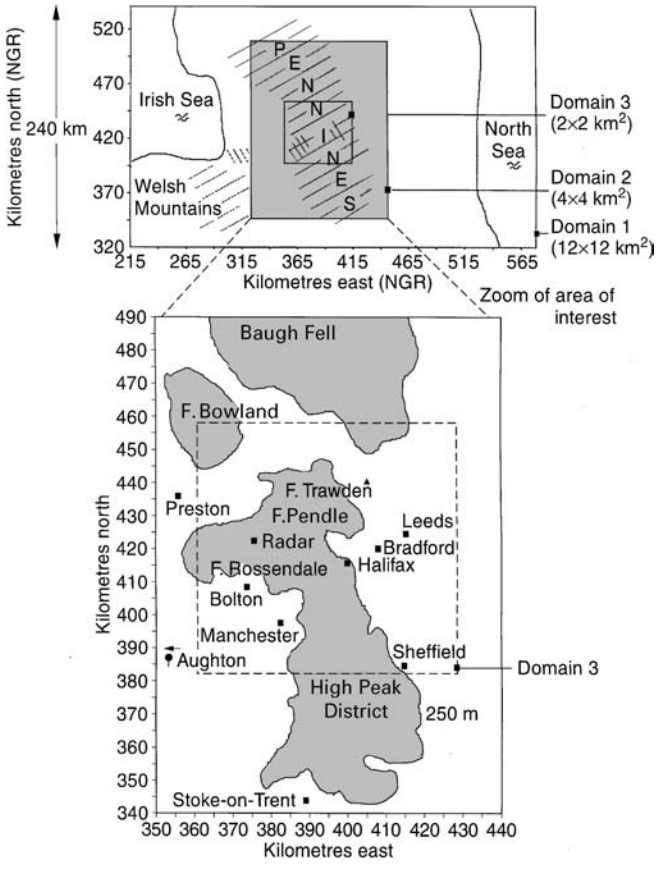

Fig. 1. Two schematic maps of the study area and model domains. The axes use standard national UK grid references

understanding of the circumstances leading to these storms. Miller (1978), for example, simulated the Hampstead storm which caused much damage in the London area on 14 August 1975. Brugge and Moncrieff (1992) investigated the devastating Munich storm from 12 July 1884, and showed that its dynamical structure was unusual for mid-latitude levels and probably a result of strong low-level relative flow. The simulation of the Halifax storm (Swann, 1993) showed that the tendency of the storm to deviate to the right of the mid-tropospheric winds could be reproduced. Wilhelmson and Klemp have done much research on the simulation of convective storm dynamics (e.g. Klemp and Wilhelmson, 1978a, b; Wilhelmson and Klemp, 1981). In particular, they have addressed the simulation of the splitting of severe convective storms, an often observed feature. Larger scale organised convective systems, such as squall lines, have been investigated for example by Lafore and Moncrieff (1989), and more recently by Caniaux *et al.* (1995), who addressed the interaction between the meso-γ-scale convective cells and the meso-β-scale stratiform region. They have found that the pressure field plays an important role in organising the inner circulation of the convective structures.

Many studies have been performed to understand the dynamics and internal organisation of convective storms. Farley and Orville (1986) for example simulated many observed features of severe hailstorms including sloping updraughts, domed tops, recycled precipitation, and moving gustfronts. Wilhelmson and Klemp (1978) demonstrated that the magnitude of the low-level shear affected the development and propagation of convective storms. On a larger scale, Schlesinger (1982) could show the importance of mesoscale lifting in organising and sustaining convective storms. The initiation of convection through mechanical or thermal forcing has been addressed in many studies. Hill (1977), for example, investigated by means of a 2D model the effect of surface heating on the development of cumulus convection. Clark and Gall (1982) investigated the airflow over different types of mountainous terrain, including simple surface differential heating, showing that the heating of slopes at elevated terrain was an important feature for the development of convection. Results of Smolarkiewicz and Clark (1985) suggested that the thermodynamical inhomogeneities generated by surface characteristics such as vegetation and soil type are especially important in the early stage of the cloud field formation; later they can influence the properties of the cloud field. For a more complete review of the present literature see for example Cotton and Anthes (1989).

The aim of this research, however, was to describe the influence of the Pennines on the outbreak of convection in a more general way, and not to simulate one particular storm or to describe one particular mechanism leading to convection.

In the next section a brief description of the model is given by the set-up of the model for the different simulations. In Sect. 3 the numerical results are presented, and a summary of results and conclusions drawn in Sect. 4.

2 Model description and set-up

2.1 Description of the Clark-model

The Clark model has previously been used successfully to investigate problems addressing the dynamic effects of air flow over complex terrain (Bruintjes *et al.*, 1994; Smolarkiewicz and Clark, 1985; Clark and Farley, 1984; Clark and Gall, 1982; Clark and Hall, 1991). The underlying theory of the model is described in detail elsewhere, for example in Clark (1979), and therefore in the following only the basic equations are given:

The Clark model is a 3D finite-difference, non-hydrostatic model, which uses a terrain-following co-ordinate transformation based on the work of Gal-Chen and Somerville (1975). The model is based on the equation of motion (see e.g. Clark, 1979)

$$\bar{\varrho}\frac{d\mathbf{V}}{dt} + 2\bar{\varrho}\boldsymbol{\Omega}\times\mathbf{V} = -\nabla p' + \mathbf{k}\bar{\varrho}g\left(\frac{\Theta'}{\bar{\Theta}} - \frac{p'}{\gamma\bar{p}}\right) + \frac{\partial\tau_{ij}}{\partial x_j} \qquad (1)$$

where ϱ is density of air, $\mathbf{V}$ is the three-dimensional wind vector, $\mathbf{k}$ is the unit vector in the vertical direction, $\boldsymbol{\Omega}$ the angular rotation vector of the Earth (the full Coriolis effects are considered in the present set-up), γ is the ratio of the heat capacities at constant pressure and constant volume (c_p/c_v), q_v stands for water vapour mixing ratio,

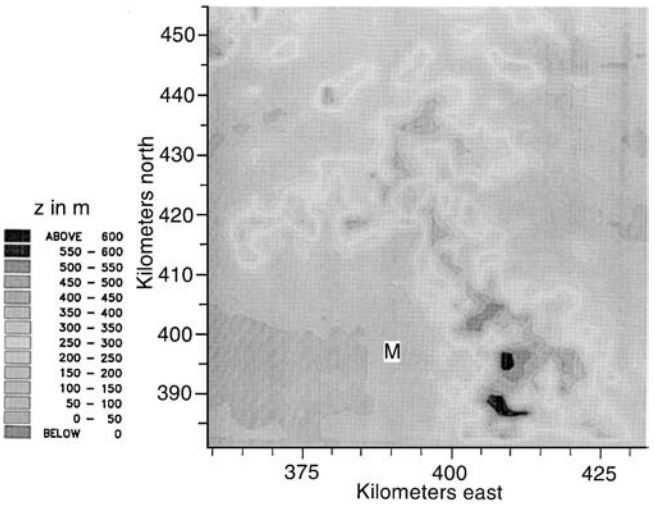

Fig. 2. Topography of the innermost domain at a resolution of $2 \times 2\,\mathrm{km}^2$. The axes use standard national UK grid references

p is atmospheric pressure, g is the gravitational constant, Θ is the potential temperature, and τ_{ij} is the stress tensor due to the subgrid-scale turbulent processes.

The mass continuity equation is used in the anelastic form (Ogura and Phillips, 1962)

$$\nabla \cdot \varrho \mathbf{V} = 0. \tag{2}$$

The equations governing heat and moisture conservation are described in great detail in Bruintjes *et al.* (1994), and are not repeated here. The rain parametrisation of the model is based on the Kessler scheme (1969), and the ice microphysics scheme on the work of Koenig and Murray (1976). The second-order-accurate positive-definite advection transport algorithm (MPDATA) of Smolarkiewicz (1984) and Smolarkiewicz and Clark (1986) was used for the conservation equations of heat and moisture.

The Clark model uses interactive two-way grid nesting procedures, which allows inclusion of several domains of different grid size resolutions. This enables the user not only to capture larger-scale flow patterns with a coarse resolution, but also to focus in detail on an area of interest. In the outermost domain an approximation to free-slip boundary conditions for the velocity components and zero-flux-type conditions on all thermodynamic variables are employed at the upper boundaries. Reflection of waves at the upper lid of the domain are treated with a Rayleigh damping and Newtonian cooling sponge layer above the layer of grid nesting.

2.2 Initialisation and set-up of the simulations

The model was set up with three nested domains as indicated in Fig. 1 with grid resolutions of $12 \times 12\,\mathrm{km}^2$, $4 \times 4\,\mathrm{km}^2$, and $2 \times 2\,\mathrm{km}^2$. The vertical grid resolution was 1 km throughout all domains, a limitation imposed by the restriction of computing time. Quantitative analysis requires a finer horizontal and vertical resolution to resolve the small-scale turbulent processes accurately (Doms and Herbert, 1985), and therefore the analysis was largely qualitative. The outermost extended up to 24 km, the two inner domains up to 16 km. The outermost domain of the model covered an area of roughly $500 \times 250\,\mathrm{km}^2$, the second domain of $150 \times 100\,\mathrm{km}^2$, and the third domain $70 \times 70\,\mathrm{km}^2$. The chosen time step was 20 s.

The topography for the inner domains was obtained from the UK Meteorological Office at a resolution of $500 \times 500\,\mathrm{m}^2$, data for the outer domain was extracted normally from Ordnance Survey maps at 5 km steps. Both data sets were combined to a homogeneous data set of 1×1 km resolution using a bi-linear distance weighting interpolation routine. The topography of the innermost domain is shown in Fig. 2 at the resolution of $2 \times 2\,\mathrm{km}^2$ used in the simulations. An Ekman friction layer was applied at the surface. A simple xy-dependent feedback, μ, between soil and atmosphere was introduced in the formulation of the sensible heat flux, S_s, as developed from Clark and Gall (1982).

$$S_s = \mu(x, y) S_0 (\cos Z - h_x \cos\delta \sin H - h_y [\sin\varphi \cos\delta \cos H - \cos\varphi \sin\delta]) \times \frac{1}{\sqrt{1 + h_x^2 + h_y^2}}, \tag{3}$$

where $\mu(x, y)$, a conversion rate from incoming solar radiation to sensible heat flux, allows the surface sensible heat fluxes to vary accordingly to the soil type distribution. S_0 is the solar constant (1395 Wm^2), Z is the Sun's zenith angle, φ latitude, δ declination angle, H hour angle, and h_{xy} are the gradients of topography in the east and north direction respectively. The estimates for this conversion rate, μ, varied around an average of 30%. Over urbanised areas (villages, cities) it varied between 30–35%, and over moist surfaces (parks, rivers, moors) between 25 and 30%. The occupation of the soil was extracted from Ordnance Survey maps. Over sea the conversion rate was set to nearly zero, resulting in temperature gradients from sea to land. The subsequently generated sea breezes produced converging winds at the Pennines. The latent flux was calculated with a constant Bowen ratio of 1. All simulations presented in the following were initialised with the same set-up of topography, influence of urban heat islands, and sea breezes. After 3 h of convective activity feedback from long-wave radiation and surface heat fluxes would become effective, which was not accounted for in the present model set-up. Therefore, data of longer than 240 min were not considered.

The model was set-up with one single profile of pressure, temperature, humidity and winds (Fig. 3). The profile chosen for the initialisation was typical for the week 19–24 May 1989, a period of widespread convective activity all over the British Isles. In this week several intense thunderstorms developed in the north of England (Collinge *et al.*, 1990; Acreman, 1989) of which three were studied in great detail (Thielen, 1994). Although it was not intended to simulate one particular storm, whenever possible, the winds in the model were initialised realistically so that the numerical data could qualitatively be compared with the observational data. All simulations were set-up with unidirectional wind shear. However, due to the

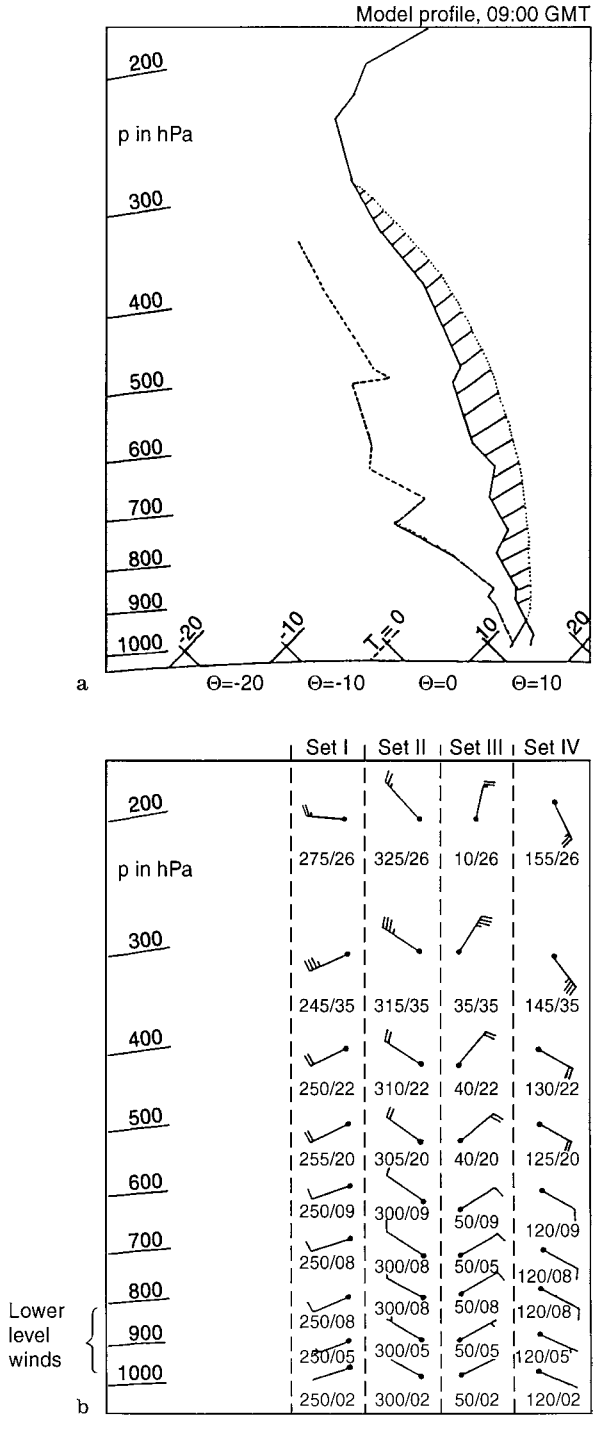

Fig. 3. a Initialisation profile of dew point and dry bulb temperatures for the numerical simulations. The *shaded area* represents the convectively available potential energy (CAPE) of the air masses. **b** Profiles of wind vectors given in degrees and knots

developing sea breeze, the model developed directional wind shears in the lower levels.

3 Model results

All model simulations were started at a time corresponding to 0900 UT, in order to give the model a sufficiently long start-up time to generate its own flow. The spin-up time of this model was about 30 min. All times refer to the starting time of 0900 UT.

3.1 Simulations with winds of westerly direction

SET I was set-up with southwesterly winds throughout the atmosphere, while in SET II the winds were north-westerly. In both simulations a sea breeze had developed after 2 h, and caused weak converging winds around the Pennines (Fig. 4).

Temporal development. Figures 5 and 6 show the rainwater mixing ratios in 2 km height for the first two sets. In SET I the convection was initiated mostly in the east of the Pennines (outlined terrain higher than 250 m), thus in the lee of the ridge (Fig. 5a). After 165–180 min (Fig. 5b, c), the convection along the windward slopes started to develop, to intensify and to result in persistent convection throughout the inner domains. Similar initial patterns occurred in SET II, which was set-up with north-westerly winds. Figure 6a shows the rainwater mixing ratio after 165 min for SET II, and again most convection started in the lee of the Pennines. Thirty minutes later (Fig. 6b) convection on both sides of the Pennines had developed, generally leaving a convection-free zone over the top of the ridge.

The initiation of cells along the leeward slopes occurred 15–30 min prior to the outbreak of cells windward of the ridge. Since during the whole morning the leeward slopes were Sun facing, it seemed that these cells could at least partly be caused by increased buoyancy (fields not shown); the forced lifting along the western slopes being a less effective trigger mechanism. Considering the moderate height of the Pennines (up to 800 m) this result is not surprising as forced lifting would produce updraughts of the order of cm/s, while temperature gradients of a few degrees C could cause updraughts of several m/s.

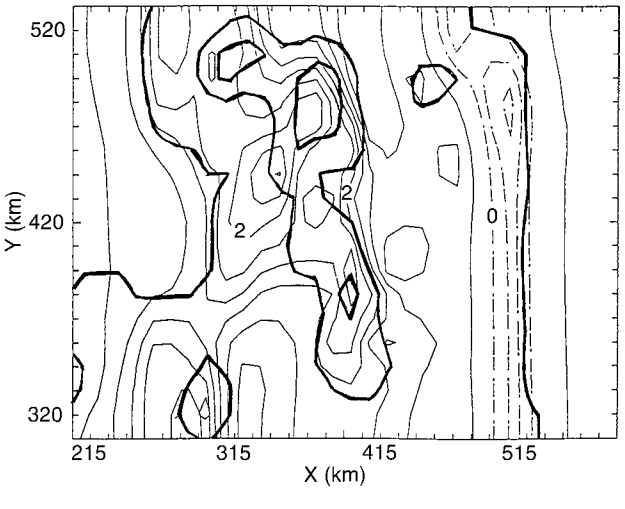

Fig. 4. Surface u_x field in m/s after 120 min for SET I, contour line interval 0.5 m/s. The topography is outlined in *bold* at intervals of 175 m

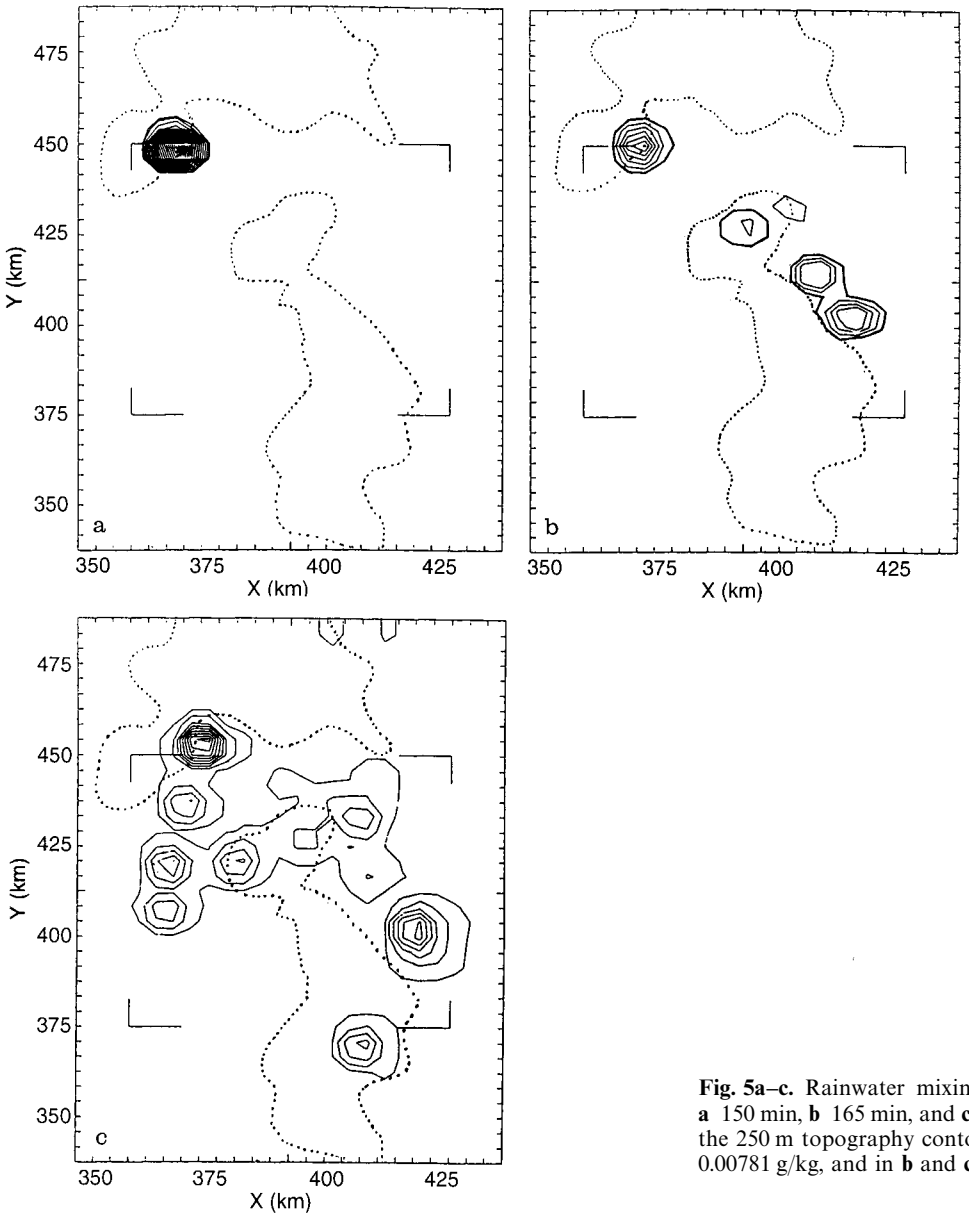

Fig. 5a–c. Rainwater mixing ratio, q_R, at 2 km for SET I after **a** 150 min, **b** 165 min, and **c** 180 min. The *dotted outline* represents the 250 m topography contour line. The q_R *contour interval* in **a** is 0.00781 g/kg, and in **b** and **c** 0.0625 g/kg

A summary of the convective developments in the inner domains is represented by overlaying the 0.0625 g/kg q_R-contour lines at 2 km of all time steps (this contour signified the beginning of first convective rain development). The overlay then indicates which areas were affected by convection during each simulation. Elevated terrain of higher than 250 m is stippled (Fig. 7a, b). The times of the tracings are indicated in the diagrams.

Spatial distribution. Summarising the results from Fig. 7a, b, it appeared that winds with a westerly component forced the creation of cells along both sides of the Pennines, leaving a mostly convection-free corridor upwind of the western slopes of the Pennines. The only exception was in the vicinity of the Forest of Trawden and Forest of Rossendale, where convection seemed to 'bridge' from west to east also on high ground. In both SETS, the area of Greater Manchester (M) appeared to be sheltered from convection under the given meteorological conditions, whereas the area around Bradford was affected by convective cells in both simulations. Under influence of northwesterly winds, the convection was slightly stronger and more widespread than under influence of southwesterly winds.

3.2 Simulations with easterly wind components

Simulation SET III was initialised with northeasterly winds throughout the atmosphere, and SET IV with southeasterly winds. As in the two previously described runs, in both cases there was no directional wind shear between lower and upper levels, except for the shear induced by a sea breeze.

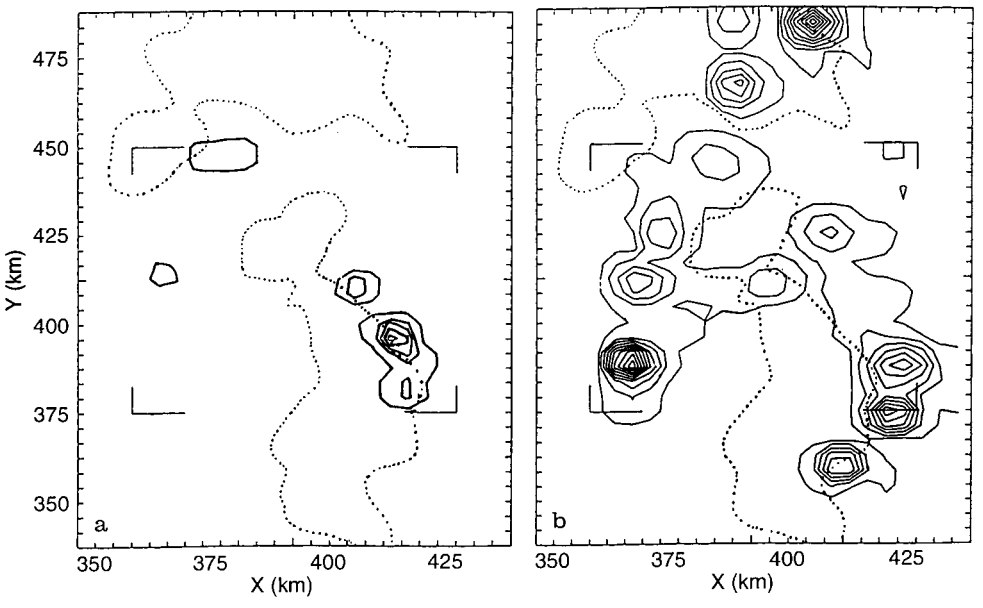

Fig. 6a, b. Rainwater mixing ratio, q_R, at 2 km height for SET II after **a** 165 min, and **b** 195 min. The *dotted outline* represents the 250 m topography contour line. The q_R *contour intervals* are 0.0625 g/kg in both diagrams

Temporal development. With easterly winds the easterly slopes were both Sun facing and upwind of the flow during the morning. One could therefore have expected convection to be initialised along the eastern slopes first. However, also in SET III and SET IV, convection was also initiated in the lee of the Pennines, along the western slopes. Only after a further 15–30 min did new cell development additionally occur along the eastern, upwind, slopes. This indicates that at least one trigger mechanism other than increased buoyancy or forced lifting at Sun facing slopes must have been present. Flow even over moderate hills can affect the mean flow in many different ways and over a great range of length and time scales (Carruthers and Hunt, 1990), and perturb the airflow in the lee of the obstacle. Under favourable meteorological conditions, when the Scorer parameter decreases with height, lee waves can develop (Beer, 1974). Although the presence of lee waves could not be proved, indications of perturbations of the flow in the lee of the hills could be found in the simulations (Fig. 8), and suggested that lee perturbations might have acted as a source of convective instability; the effects of increased buoyancy and forced lifting could be considered as acting comparatively slowly. This will be addressed in another study with a more detailed grid spacing by Thielen later.

Spatial distribution. The summaries of SET III and SET IV (Fig. 9a, b) show different convection patterns than Fig. 7a, b. Winds with easterly wind components resulted in a convection-free corridor which was aligned in SE/NW direction. Again the areas upwind of the (eastern) slopes appeared to exhibit less convection, whilst convection was concentrated to the west of the Pennines. Consequently, Manchester was strongly affected by convection in these simulations.

The 'bridge' of convection from east to west around the elevated terrain of the Forest of Trawden and Forest of Rossendale was also present in SET III, but not pronounced in SET IV. Sensitivity tests on the influence of urban heat islands in the simulation showed, that convection was generally enhanced downwind of the two large urban areas Manchester and Bradford/Leeds (Thielen, 1994). Consequently, under influence of southwesterly and northeasterly wind directions, this particular region of the central Pennines are in a favourable position for convective activity, because they are downwind of one of the major urban areas (downwind of Manchester for southwesterly flow, downwind of Bradford/Leeds for northeasterly flow). In case of southeasterly flow, the combination of lee perturbations and enhanced convection downwind of urban areas resulted in outbreak of cells to the north of the Forest of Trawden. It is also possible that the structured terrain in this area might have played a role, but, again, simulations on a higher resolution would be necessary to investigate this further.

3.3 Overall structure of convective storms in the study area

In all simulations the outbreaking convection was of multi-cellular nature (Thielen, 1994), a feature that could also be observed in the radar data (see Collinge *et al.*, 1990). Cells generally appeared to be short lasting, but because the output of numerical data was mostly only produced in 15 minute steps, no definite conclusions on cell duration lifetime less than this, could be made. Analysis of a few runs with a higher output frequency (not shown), as well as analyses of data from the Hameldon Hill C-band weather radar (Table 1) seemed to suggest that convective cells in the assumed conditions lasted for time periods of 10–20 min. In the radar data many cells with lifetimes of 5 min only were observed (Thielen, 1994).

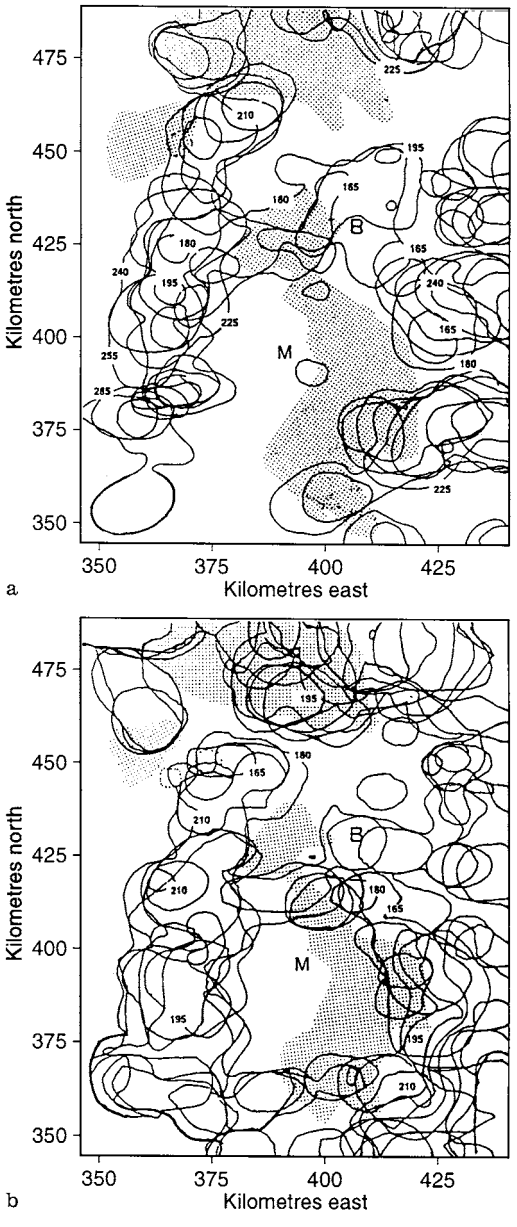

Fig. 7a, b. Overlay of the 0.0625 g/kg contours of rainwater mixing ratio (q_R); elevations over 250 m are stippled. *M* and *B* refer to Manchester and Bradford/Leeds respectively. The *numbers* indicate the time in minutes of outbreak of cells for SET I **a** and SET II **b**

Once cells were triggered they mostly moved in direction of the 700–800 hPa mean winds, in accordance with other observations and simulations (e.g. Newton and Frankhauser, 1975; Thorpe and Miller, 1978). Both deviations to the right or to the left of these winds were simulated, but no preferred deviation direction could be determined. In the observational data persistent deviations to the right of the mean 700–800 hPa layer winds could be seen during the Halifax storm (Collinge *et al.*, 1990), while the example on 24 May 1990, both deviation to the right and to the left of these winds occurred (Thielen, 1994). It appeared as if at some places, for example the High Peak district, the deviation could have been related to the underlying terrain, but simulations at

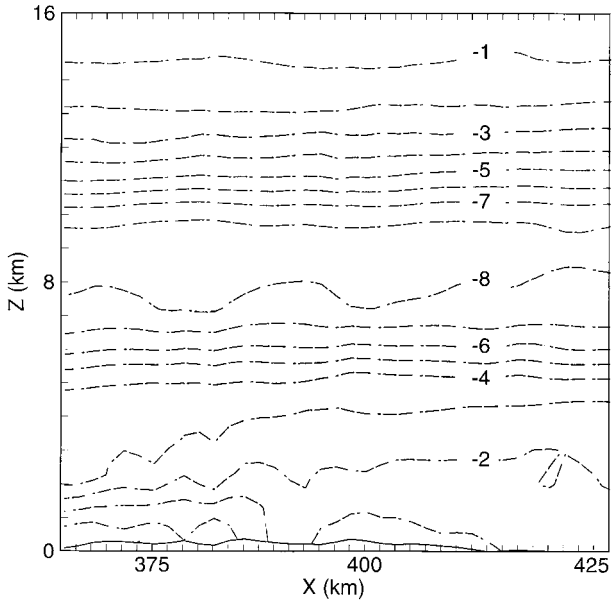

Fig. 8. *xz* cross section of the horizontal wind component u_x for the inner model domain at 415 km North (NGR) at 120 min. The *contours* are given in m/s in 1 m/s intervals. The surface topography is *outlined*

finer grid resolutions would have to be performed to draw more definite conclusions.

3.4 Comparison with observational results

Most of the storms listed in the introduction developed under the influence of southwesterly winds, the prevailing winds in this region. In Fig. 10, wind profiles and storm totals of three storms that developed during southwesterly winds, and of one that developed during northeasterly winds are shown.

The first part of the figure shows an overlay of the radar estimated storm totals of the Halifax storm (dashed lines), and of the Toddbrook storm and the Ribble Valley storms, which developed on 24 May 1989. Qualitative comparison between the simulation in SET I (Fig. 7a) and the storms in Fig. 10a, shows reasonable agreement of the areas affected by convection. Both figures show (1) a convection-free corridor southwest of Manchester, (2) two bands of convective activity along (a) the eastern slopes of the Pennines, and (b) 25 km upwind of the western slopes of the Pennines, (3) a 'bridge' of convection in the central Pennines.

Figure 10b shows the storm totals of the Hewenden Reservoir storm, which developed on 11 June 1956, and for which only gauged rainfall data was available. Consequently, the spatial distribution of the rainfall is less certain than for the other storms. It is also possible, that there was rainfall outside of the gauge network used for this study. Although this comparison is based on a single storm only, the location of the event agrees well with accumulation of cells simulated in the central Pennines (Fig. 9a).

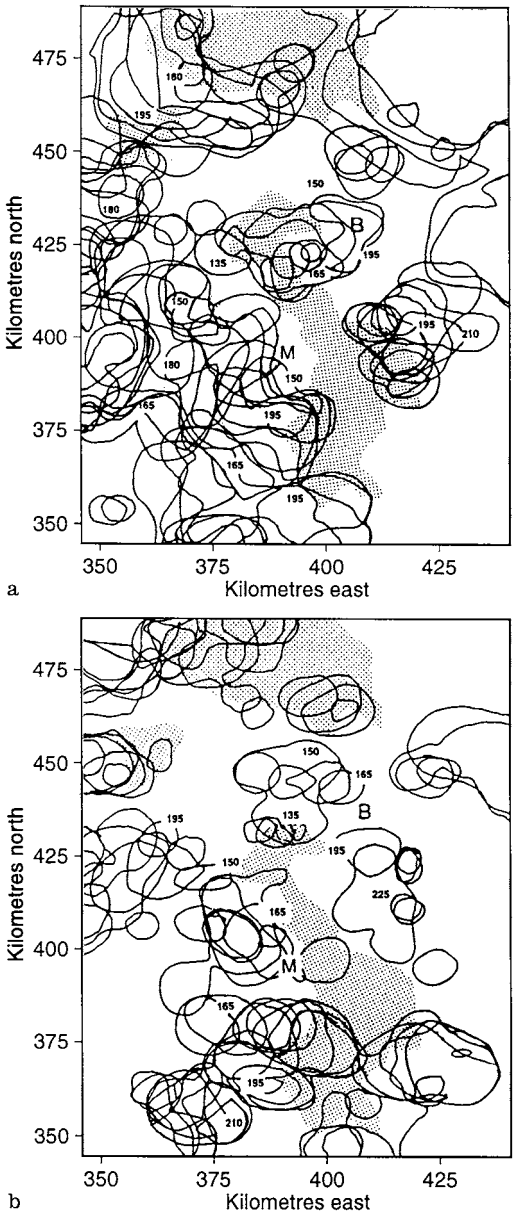

Fig. 9a, b. Overlay of the 0.0625 g/kg contours of rainwater mixing ratio (q_R); elevations over 250 m are *stippled*. *M* and *B* refer to Manchester and Bradford/Leeds respectively. The *numbers* indicate the time in minutes of outbreak of cells for SET III **a** and SET IV **b**

Table 1. Percentage (%) occurrence of individual cells with rainfalls higher than 10 mm/h during three different storm events that took place in the area of study in the week 19–25 May 1989

Time in Min.	1–10	11–20	21–30	31–40	41–50	>51
Halifax storm (19 May 1989)	59	24	8	8	1	0
Toddbrook storm (24 May 1989)	54	35	10	1	0	0
Ribble Valley Storm (24 May 1989)	36	26	24	8	2	4

Obviously, quantitative comparisons were not possible, since the crude resolution of the model did not allow realistic rainfall quantities to develop. Thus, on the basis of the presented data the model results could not be validated or asserted. However, overall the observations seemed to confirm the presence of areas with an increased likelihood for the outbreak of convection under certain wind directions.

5 Summary of results and conclusions

Analyses of the numerical results presented suggest that for those winds not parallel to the ridge, convection is initiated in the lee of the elevated terrain, independent of the inflow direction and the exposure of the slopes to the Sun. Only after a time delay of 15–30 min can cell formation upwind of the slopes be expected. This suggested that perturbation of the air flow in the lee of the ridge could act as an effective faster trigger mechanism than the increased buoyancy along Sun facing slopes. The influence of forced lifting seemed to be comparatively small.

In general the convection occurred to the east and the west of the north-south extending ridge, leaving the ridge tops largely convection-free. An exception to this was found in the elevated terrain of the central Pennines area, the Forest of Trawden, the Forest of Pendle, and the Forest of Rossendale. In this region and on top of this ridge, rain developed in most simulations, giving the impression that the rainfall was 'bridging' from one side of the Pennines to the other. This is supported in general by observations, gauge and radar data (Collinge *et al.*, 1992; Collinge *et al.*, 1994), e.g. the Halifax storm with a total of 193 mm in 2 h, and the Hewenden Reservoir storm with a total of 155 mm in 105 min. It was assumed that the focusing of convection in this area was due to a combination of different mechanisms such as lee perturbations, enhancement of convection downwind of urban areas, and increased buoyancy along Sun-facing slopes. Their relative importance depending on different wind directions and possibly the influence of special topography in this region, should be addressed in further studies with a more suitable grid mesh for fine-scale processes.

Analyses of the observational data had indicated, that storms in the north of England tended to have multicellular character with relatively short-lived cells. A large number of cells lasted only for a 10 min period, particularly during the Halifax storm on 19 May 1989 (Collinge *et al.*, 1992). Similarly, the numerical simulations also produced short-lived cells of 15 min or less duration, but due to limited computer resources, no finer time scale can be produced.

When simulating convective storms one has to be aware that they are characterised by a maximisation of atmospheric processes, such as exceptionally high up- and down-draughts, extreme variations in the droplet spectrum, and growth of very large hail particles. Their parametrisations, on the other hand, are mostly derived from mean values, and may therefore not be able to describe strong convective processes adequately. Grid nesting was used to resolve interactive processes on relatively small scales with larger scale dynamical processes. However, imposed by limited computer time resources, the necessary grid resolution to resolve microphysical processes

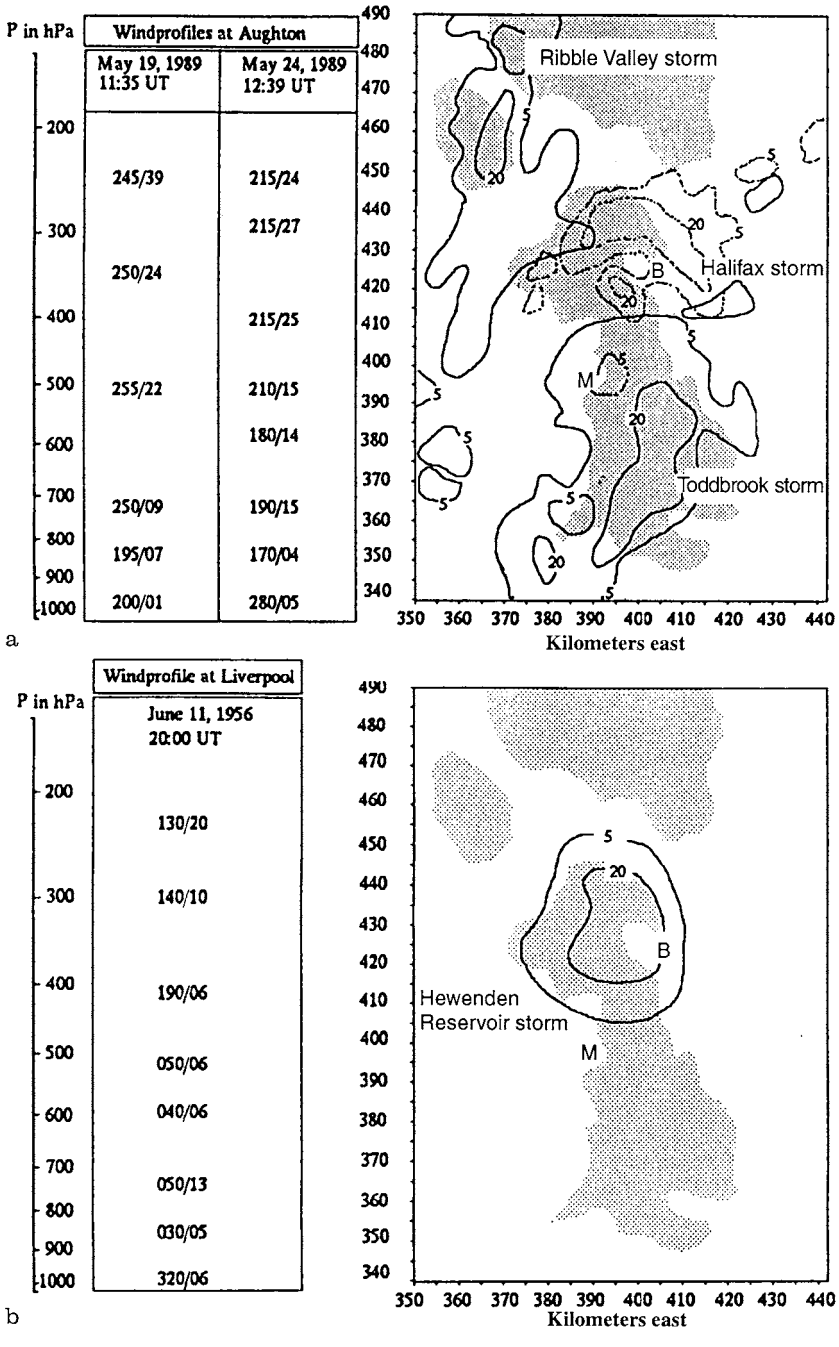

Fig. 10a, b. Wind profiles with height and storm totals of **a** three storms that developed during southerly to southwesterly winds. The *contours* for those storms that developed on 24 May 1989 are drawn in *solid lines*, those for the storm on 19 May 1989 in *dashed lines*, **b** one storm that developed during northeasterly flow. The 5 mm and 20 mm *isohyets* are drawn, the wind directions are given in *degrees* and the speed in *knots*

and their interaction with subgrid turbulent processes (length scales of the order of 100 m, Doms and Herbert, 1989), were not possible, and thus no quantitative analysis could be performed.

In the present coupled model the soil has been parametrised only crudely for the latent and sensible heat fluxes, and these parametrisations remained constant during the whole simulations. For a more realistic coupling, an independent and more complex soil module, calculating heat and moisture fluxes depending on water balances within the soil at each time step, should be introduced (see, e.g. Noilhan and Planton, 1989).

Acknowledgements. The authors would like to thank T. Clark and W. Hall for providing the model code and advice for this study, J. F. R. McIlveen and R. Lord for discussion of the results, the NERC (GR9/814) for granting computing time on the YMP-8 at the Rutherford Appleton Laboratories, and the EC (CEC 900898) for financial support.

The Editor-in-Chief thanks two referees for their help in evaluating this paper.

References

Acreman, M., Extreme rainfall at Calderdale, 19 May 1989, *Weather*, **44,** 438–446, 1989.

Baser, M. J., C. G. Collier, and F. F. Hill, Radar and rain-gauge observations near Manchester: 5/6 August 1981, *Meteorol. Mag.*, **112,** 149–162, 1983.

Beer, T., *Atmospheric waves*, Adam Hilger, 1974.

Brugge, R., and M. W. Moncrieff, Multi-cell stage of the Munich storm of 12 July 1984: a numerical study, *Tellus*, **44,** 339–355, 1992.

Bruintjes, R. T., T. L. Clark, and W. D. Hall, Interactions between topographic airflow and cloud/precipitation development during the passage of a winter storm in Arizona, *J. Atmos. Sci.*, **51(1),** 48–67, 1994.

Caniaux, G., J.-P. Lafore, and J.-L. Redelperger, A numerical study of the stratiform region of a fast-moving squall line. Part II: relationship between mass, pressure, and momentum fields, *J. Atmos. Sci.*, **52(3),** 331–352, 1995.

Carruthers, D. J., and J. C. R. Hunt, Fluid mechanics of airflow over hills: turbulence, fluxes, and waves in the boundary layer, *Atmospheric Processes over Complex Terrain, Meteorol. Monogr.*, Amn. Meteorol. Soc., 1990.

Chaplain, H. R., Record rainfalls in Leeds and West Yorkshire during June 1982, *Weather*, **37(10),** 282–286, 1983.

Clark, T. L., Numerical simulations with a three-dimensional cloud model: lateral boundary condition experiments and multicellular severe storm calculations, *J. Atmos. Sci.*, **34,** 2191–2215, 1979.

Clark, T. L., and D. Farley, Severe downslope windstorm calculations in two and three spatial dimensions using anelastic interactive grid nesting: a possible mechanism for gustiness, *J. Atmos. Sci.*, **41,** 329–350, 1984.

Clark, T. L., and R. Gall, Three-dimensional numerical simulations of airflow over mountainous terrain: a comparison with observations, *Mon. Weather Rev.*, **110,** 766–791, 1982.

Clark, T. L., and W. D. Hall, Multi-domain simulations of the time dependent Navier-Stokes equations: benchmark error analysis of some nesting procedures, *J. Comp. Phys.*, **92(2),** 456–481. er, Vol. 44, 1991.

Collinge, V. K., and M. Acreman, The Calderdale storm revised: an assessment of the evidence, *BHS 3rd National Hydrology Symposium*, Southampton, 1991.

Collinge, V. K., E. J. Archibald, K. R. Brown, and M. E. Lord, Radar observations of the Halifax storm, 19 May 1989, *Weather*, **45(10),** 354–365, 1990.

Collinge, V. K., J. Thielen, and J. F. R. McIlveen, Extreme rainfall at Hewenden Reservoir, 11 June 1956; *Meteorol. Mag.*, 1440, **121,** 166–171, 1992.

Cotton, W. R., and R. A. Anthes, *Storm and cloud dynamics*, Academic Press, San Diego, California, 1989.

Dent, L., and G. Monk, Large hail over Northwest England, 7 June 1983; *Meterol. Mag.*, 1346, **113,** 249–265, 1983.

Doms, G., and F. Herbert, Fluid- und Mikrodynamik in numerischen Modellen konvektiver Wolken, *Ber. Inst. Meteorol. Geophys. Univ. Franfurt/Main*, Eigenverlag des Institutes, **62,** 1985.

Farley, R. D., and H. D. Orville, Numerical modeling of hailstorms and hailstone growth, *J. Clin. Appl. Meteorol.*, **25,** 2014–2035, 1986.

Gal-Chen, T., and R. C. J. Somerville, On the use of a coordinate transformation for the solution of the Navier-Stoke Equation, *J. Comp. Phys.*, **17,** 209–228, 1975.

Hill, G. E., Factors controlling the size and spacing of cumulus convection, *J. Atmos. Sci.*, **34,** 1934–1941, 1977.

Kessler, E., On the distribution and continuity of water substances in atmospheric circulations, *Meteorol. Monogr.*, **32,** 84pp, 1969.

Klemp, J. B., and R. B. Wilhelmson, The simulation of three-dimensional convective storm dynamics, *J. Atmos. Sci.*, **35,** 1070–1096, 1978a.

Klemp, J. B., and R. B. Wilhelmson, Simulations of right- and left-moving storms produced through storm splitting, *J. Atmos. Sci.*, **35,** 1097–1115, 1978b.

Koenig, L. R., and F. W. Murray, Ice-bearing cumulus cloud evolution, Numerical simulation and general comparison against observation, *J. Appl. Meteorol.*, **15,** 747–762, 1976.

Ludlam, F. H., *Clouds and storms, the behaviour and effect of water in the atmosphere*, Pennsylvania State Press, 1980.

Miller, M. J., The Hampstead storm: a numerical simulation of quasi-stationary cumulus nimbus systems, *Q. J. R. Meteorol. Soc.*, **104,** 413–427, 1978.

Moncrieff, M.W., The dynamical structure of two-dimensional steady convection with constant vertical shear, *Q. J. R. Meteorol. Soc.*, **104,** 543–567, 1978.

Newton, C. W., and C. J. Frankhauser, Movement and propagation of multi-cellular convective storms, Pageoph, Vol. 113, Birkhäuser, Basel, 1975.

Noilhan, J., and S. Planton, A simple parameterisation of land surface processes for meteorological models, *Mon. Weather Rev.*, **117,** 536–549, 1989.

Ogura, Y., and A. Phillips, Scale analysis of deep and shallow convection in the atmosphere, *J. Atmos. Sci.*, **19,** 173–179, 1962.

Reynolds, G., Maximum precipitation in Great Britain, *Weather*, **33(5),** 162–166, 1978.

Schlesinger, R. E., Effects of mesoscale lifting, precipitation and boundary layer shear in severe storms dynamics in a 3D numerical modeling study, *Preprints, 12th Conference on Severe Local Storms, AMS*, Boston, pp. 536–541, 1982.

Smolarkiewicz, P. K., A fully multidimensional positive definite advection transport algorithm with small implicit diffusion, *J. Comp. Phys.*, **54,** 325–362, 1984.

Smolarkiewicz, P. K., and T. L. Clark, Numerical simulation of the evolution of a three-dimensional field of cumulus clouds, Part I: model description, comparison with observations and sensitivity studies, *J. Atmos. Sci.*, **42(5),** 502–522, 1985.

Swann, H., Modelling convective systems on the large eddy simulation model, *Internal Report, Joint Centre for Mesoscale Meteorology*, Newsletter, **4,** Feb. 1993.

Thielen, J., The influence of the Pennines on severe convective storms; a study by radar observation and modelling, PhD thesis at the Environmental Science Department at Lancaster University, 1994.

Thorpe, A., and M. Miller, Numerical simulations showing the role of downdraughts in storm propagation and storm splitting, *Q. J. R. Meteorol. Soc.*, **104,** 873–893, 1978.

Wilhelmson, R. B., and J. B. Klemp, A numerical study of storm splitting that leads to long-lived storms, *J. Atmos. Sci.*, **35,** 1974–1986, 1978.

Wilhelmson, R. B., and J. B. Klemp, A three-dimensional simulation of splitting severe storms on 3 April 1964, *J. Atmos. Sci.*, **38,** 1558–1580, 1981.